

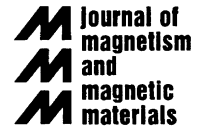


ELSEVIER

Available online at www.sciencedirect.com

SCIENCE @ DIRECT®

Journal of Magnetism and Magnetic Materials 267 (2003) 300–306

www.elsevier.com/locate/jmmm

Charge order to two-dimensional metal crossover in $\text{Pr}_{0.5}(\text{Sr}_{1-y}\text{Ca}_y)_{0.5}\text{MnO}_3$

V.N. Smolyaninova^{a,c,*}, Amlan Biswas^a, C. Hill^a, Bog-Gi Kim^b,
S.-W. Cheong^b, R.L. Greene^a

^aDepartment of Physics and Center for Superconductivity Research, University of Maryland, College Park, MD 20742, USA

^bDepartment of Physics and Astronomy, Rutgers University, Piscataway, NJ 08854, USA

^cDepartment of Physics, Astronomy and Geosciences, Towson University, 8000 York Road, Towson, MD 21252, USA

Received 4 February 2003; received in revised form 25 April 2003

Abstract

We report a low-temperature specific heat study of $\text{Pr}_{0.5}(\text{Sr}_{1-y}\text{Ca}_y)_{0.5}\text{MnO}_3$ ($0 < y < 1$) as it changes from charge-ordered insulator ($y = 1$) to AFM 2D metal ($y = 0$). A two-phase coexistence for the intermediate compositions is found. The effect of magnetic field on the specific heat of $\text{Pr}_{0.5}\text{Sr}_{0.5}\text{MnO}_3$ is also presented and discussed.

© 2003 Elsevier B.V. All rights reserved.

PACS: 75.30.Vn; 71.30.+h; 75.50.Cc; 75.40.Cx

Keywords: Manganites; Charge ordering; Phase separation

1. Introduction

Doped rare-earth manganites $\text{R}_{1-x}\text{A}_x\text{MnO}_3$, (R being a trivalent rare earth and A being a divalent alkaline-earth ion) exhibit a large diversity in electronic, magnetic, and orbital states due to the complex interplay of the corresponding degrees of freedom. One of the most intriguing properties of manganites is charge ordering (CO), where holes are localized at fixed positions of the Mn^{4+} ions. At $x = 0.5$ several compounds, such as $\text{La}_{0.5}\text{Ca}_{0.5}\text{MnO}_3$, $\text{Nd}_{0.5}\text{Sr}_{0.5}\text{MnO}_3$,

$\text{Pr}_{0.5}\text{Ca}_{0.5}\text{MnO}_3$, exhibit the so-called CE-type CO. Here the Mn^{4+} and Mn^{3+} ions order, with $d_{3x^2-y^2}$ and $d_{3y^2-x^2}$ orbitals of Mn^{3+} alternatively arranged, and spins ordered in a CE antiferromagnetic (AFM) structure [1,2]. As the one-electron bandwidth increases, manganites of $x = 0.5$ composition ($\text{Pr}_{0.5}\text{Sr}_{0.5}\text{MnO}_3$, $\text{Nd}_{0.45}\text{Sr}_{0.55}\text{MnO}_3$) become charge disordered, have $d_{x^2-y^2}$ orbital state and have A-type AFM spin ordering along the z direction. The spins are ferromagnetically ordered in the x - y plane [2–4]. This orbital orientation and ferromagnetic (FM) ordering within the x - y planes promotes conduction in these planes via the double-exchange mechanism, while in the z direction electronic transport is prohibited, which makes these materials two-dimensional (2D) metals [2,3].

To better understand the physics of $x = 0.5$ manganites, it is important to know the ground

*Corresponding author. Department of Physics, Astronomy and Geosciences, Towson University, 8000 York Road, Towson, MD 21252, USA Tel.: +1-410-704-2608; fax: +1-410-704-3511.

E-mail address: vsmolyaninova@towson.edu (V.N. Smolyaninova).

state of these materials as a function of the one-electron bandwidth. The low-temperature specific heat, carrying information about principal excitations, in combination with resistivity and magnetization data is an appropriate tool for such study.

In this paper, we report a specific heat study of $\text{Pr}_{0.5}(\text{Sr}_{1-y}\text{Ca}_y)_{0.5}\text{MnO}_3$ ($0 < y < 1$) as it changes from CO insulator ($\text{Pr}_{0.5}\text{Ca}_{0.5}\text{MnO}_3$) through 2D AFM metal ($\text{Pr}_{0.5}\text{Sr}_{0.5}\text{MnO}_3$) to 3D metal ($\text{Pr}_{0.5}\text{Sr}_{0.5}\text{MnO}_3$ in magnetic field). The evolution of the specific heat with compositional change shows two phase coexistence in these materials. In $\text{Pr}_{0.5}\text{Sr}_{0.5}\text{MnO}_3$, the field-induced transition from 2D to 3D metal leads to a large increase of the density of states at the Fermi level.

2. Experimental details

Ceramic samples of $\text{Pr}_{0.5}(\text{Sr}_{1-y}\text{Ca}_y)_{0.5}\text{MnO}_3$ ($0 < y < 1$) were prepared by a standard solid-state-reaction technique. X-ray powder diffraction showed that all samples are single phase and good quality. The specific heat was measured in the temperature range 2–22 K by relaxation calorimetry [6]. The specific heat measurements have an absolute accuracy of $\pm 2\%$. The magnetization was measured with a commercial SQUID magnetometer. Resistivity was measured by a standard four-probe technique.

3. Results and discussion

The temperature dependence of the resistivity and magnetization of $\text{Pr}_{0.5}(\text{Sr}_{1-y}\text{Ca}_y)_{0.5}\text{MnO}_3$ ($0 < y < 1$) is shown in Fig. 1. The $y = 1$ ($\text{Pr}_{0.5}\text{Ca}_{0.5}\text{MnO}_3$) composition is insulating and AFM at low temperatures. The $y = 0$ ($\text{Pr}_{0.5}\text{Sr}_{0.5}\text{MnO}_3$) sample is FM and metallic above 120 K and becomes AFM at lower temperatures. The A-type AFM allows 2D transport within the FM layers, making the resistivity of the $y = 0$ sample significantly lower than the resistivity of $y = 1$ charge-ordered sample with CE-type AFM, but higher than its resistivity in the FM phase. These data are consistent with previous experimental results [2,7]. As the concentration of Ca increases, the

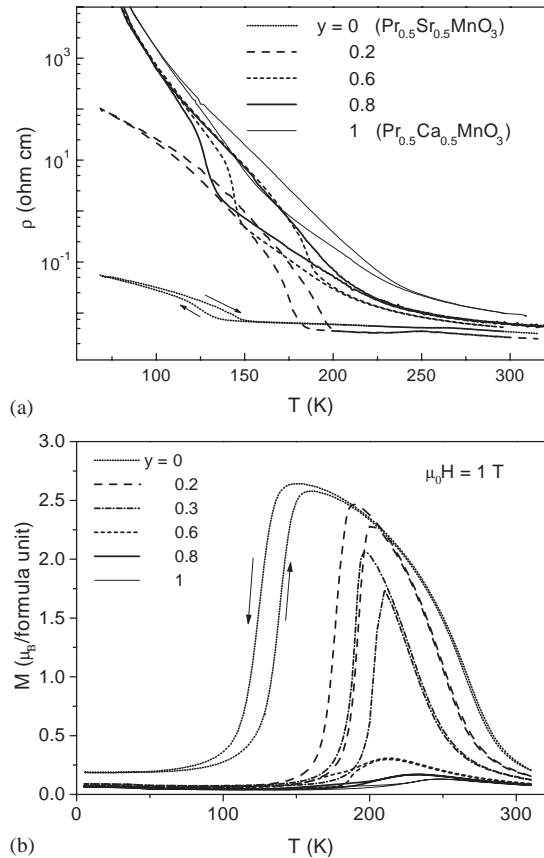


Fig. 1. Temperature dependence of the resistivity (a) and magnetization in 1 T magnetic field (b) of $\text{Pr}_{0.5}(\text{Sr}_{1-y}\text{Ca}_y)_{0.5}\text{MnO}_3$ ($0 < y < 1$). Arrows denote the cooling and warming directions.

temperature interval in which the FM phase occurs becomes narrower and the magnetization value of this phase at a given temperature decreases. This suggests a coexistence of FM and AFM phases in this temperature region, as was reported in Ref. [8]. At low temperature all compositions are AFM. The low-temperature ($T = 80$ K) resistivity values are plotted in Fig. 2a. As the concentration of Ca, y , decreases below $y = 0.3$, the low-temperature resistivity value decreases. The resistivity of the $y = 0.2$ sample is significantly lower than the higher y samples, which suggests that a highly resistive CE-type AFM CO phase coexists with a conductive A-type AFM phase at low temperatures. The

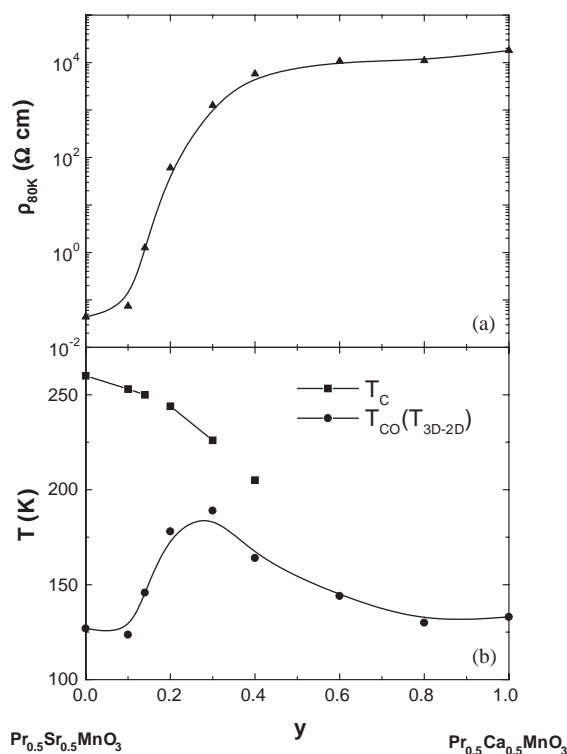


Fig. 2. (a) Resistivity value of $\text{Pr}_{0.5}(\text{Sr}_{1-y}\text{Ca}_y)_{0.5}\text{MnO}_3$ at $T = 80$ K for different y ; (b) phase diagram of $\text{Pr}_{0.5}(\text{Sr}_{1-y}\text{Ca}_y)_{0.5}\text{MnO}_3$: squares, Curie temperature (T_C); circles, the CO temperature (T_{CO}) and/or transition temperature from FM 3D metallic state to more resistive AFM 2D metallic state (T_{3D-2D}) as described in text.

phase diagram of $\text{Pr}_{0.5}(\text{Sr}_{1-y}\text{Ca}_y)_{0.5}\text{MnO}_3$ is shown in Fig. 2b. The CO temperature (for compositions with high Ca content) and the transition from FM 3D metallic state to more resistive AFM 2D metallic state (for low Ca compositions) was determined as the maximum of dR/dT on cooling. The transition temperature for intermediate compositions, determined also as the maximum of dR/dT on cooling, is most likely due to the transition to coexisting CO and AFM 2D metallic phases.

Fig. 3a shows the low-temperature specific heat of $\text{Pr}_{0.5}(\text{Sr}_{1-y}\text{Ca}_y)_{0.5}\text{MnO}_3$ ($0 < y < 1$) plotted as C/T vs. T^2 in the temperature range from 2 to 22 K. The specific heat of the samples with higher concentration of Ca ($y = 1, 0.8$, and 0.6) have anomalous excess specific heat, which manifest

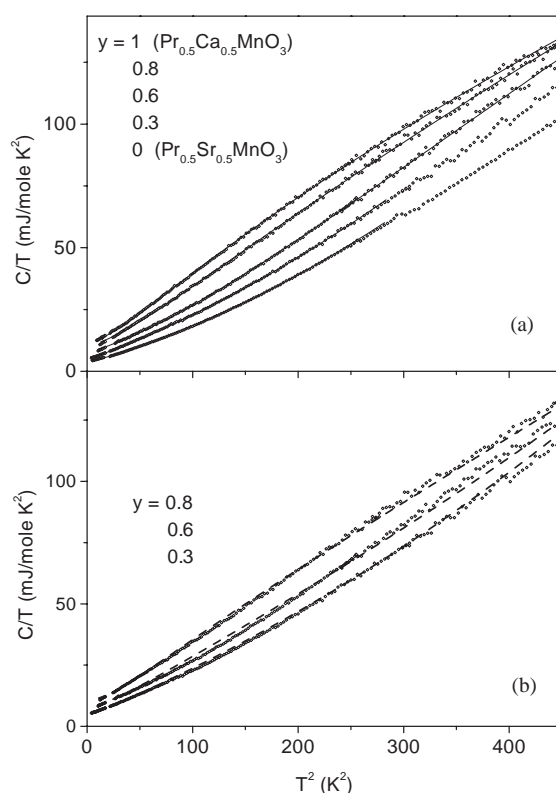


Fig. 3. Low-temperature specific heat of $\text{Pr}_{0.5}(\text{Sr}_{1-y}\text{Ca}_y)_{0.5}\text{MnO}_3$ ($0 < y < 1$) plotted as C/T vs. T^2 : (a) solid lines are fits to Eqs. (1) and (2); (b) dashed lines are fits to two-phase model. Fits are described in text.

itself as an upward curvature in the C/T vs. T^2 plot. This excess specific heat appears to be similar to what we found in CO manganites of different compositions [9–11]. We express the low-temperature specific heat of these compounds in the following form [9,10]:

$$C = \alpha/T^2 + \gamma T + \beta T^3 + C'(T). \quad (1)$$

The first term in Eq. (1) is the hyperfine contribution caused by splitting of nuclear magnetic levels of Mn and Pr ions in the field of unpaired electrons, which was observed previously in the manganites [13]. The second term in these electrically insulating samples originates from spin and charge disorder. A disordered system, which has multiple ground states, can behave as two-level systems (TLS) resulting in a specific heat

contribution proportional to the temperature [14]. A large γT term in the insulating state was found previously in CO manganites [10,15]. The third term represents the lattice and the AFM spin-wave contribution to the specific heat (The AFM spin-wave contribution to the specific heat was calculated for different magnetic structures typically resulting in a T^3 temperature dependence. This temperature dependence of AFM spin-waves was used in our fitting, since there is no other specific predictions for the CE AFM structure [16]). The last term C' is an anomalous contribution, of unknown origin, found only in the CO state in manganites with CE type of CO [9–11]. The temperature dependence of this contribution has the form of the specific heat due to nonmagnetic excitations with the dispersion relation $\varepsilon = \Delta + Bq^2$, where Δ is an energy gap and q is a wave vector: $C' = k_B V (k_B T / 4\pi B)^{3/2} (\frac{15}{4} F_{5/2}(x) + 3x F_{3/2}(x) + x^2 F_{1/2}(x))$, where $x = \Delta' / k_B T$ and $F_p(x)$ is given by $F_p(x) = \sum_{n=1}^{\infty} \frac{e^{-nx}}{n^p}$.

Using Eq. (1) we find good fits for $y = 1, 0.8$, and 0.6 compositions as shown in Fig. 3a. The fitting parameters are given in Table 1. The values of the hyperfine contribution α , are close to those found in other manganites [12,13]. However, for better accuracy in the determination of α , lower temperature measurements are required. Associated with disorder, the γ value of the insulating $y = 1$ sample is larger than what we observed in a single crystal of the same composition. The β values are typical for manganites [9,13,17,18]. The values of Δ and B , the parameters of anomalous contribution C' , are similar to those found previously in other materials [10,11]. The value of Δ (the gap value in the excitation spectrum) increases with increase of Sr content. We observed a similar increase of Δ for phase separated $(\text{Pr}_y\text{La}_{1-y})_{0.67}\text{Ca}_{0.33}\text{MnO}_3$ [11] when the volume fraction of the CO phase decreased and also upon application of a magnetic field [10,11]. Although the values of Δ are somewhat higher than the temperature range of our study ($\Delta = 24\text{--}48\text{ K}$, Table 1), C' term give a significant contribution to our specific heat: 32%, 27%, and 5% of total specific heat at $T = 8\text{ K}$ for $y = 1, 0.8$, and 0.6 samples, respectively, and even higher contribution at higher temperatures.

Table 1

Summary of the fitting results for the specific heat data

y ($\text{Pr}_{0.5}(\text{Sr}_{1-y}\text{Ca}_y)_{0.5}\text{MnO}_3$)	α	γ	β	Δ	B
1	9.9	11.4	0.121	2.06	9.52
0.8	9.9	9.7	0.159	2.59	9.36
0.6	9.9	6.8	0.170	4.15	5.79
0.3	4.4	4.5	0.159		
0	8.7	3.3	0.18		
0 ($\mu_0 H = 8.5\text{ T}$)	8.7	7.3	0.154		

The units of different quantities are: α (mJ K/mol), γ (mJ/mol K²), β (mJ/mol K⁴), Δ (meV), and B (meV Å²).

The anomalous contribution C' decreases as Sr content increases. For specific heat of Sr-rich samples, $y = 0.3$ and 0 , fit to Eq. (1) requires C' term to be set to zero. The neutron diffraction study on low Ca content sample, $\text{Pr}_{0.5}\text{Sr}_{0.41}\text{Ca}_{0.09}\text{MnO}_3$, showed that the superlattice reflection corresponding to the CO is very weak or negligible [19], which could correspond to a presence of only a very small fraction of charge-ordered material. This is in agreement with the absence of the C' contribution, since this contribution is present only in the CO state [9–11]. Therefore, we fit the $C(T)$ of these compositions to the form

$$C = \alpha/T^2 + \gamma T + AT^2 + \beta T^3 + \beta_5 T^5, \quad (2)$$

where the last term is a higher-order lattice contribution. The third term is an AFM spin-wave contribution found in some A-type AFM [12]. However, our best fit gives $A = 0$ even for the $y = 0$ sample. Apparently, the spin-wave contribution to the specific heat of this A-type antiferromagnet does not have a T^2 dependence. In the case of the $y = 0$ sample ($\text{Pr}_{0.5}\text{Sr}_{0.5}\text{MnO}_3$), the γT term could originate from an electronic charge carrier contribution, because in an A-type antiferromagnet the hopping conduction is allowed in the FM plane via the double exchange mechanism. However, even though there is no apparent source of disorder (magnetic or charge), we cannot completely rule out the contribution of disorder to the γT term. The fitting results for γ and β are listed in Table 1, and the β_5 values are 0.00028 and 0.00025 mJ/mol K⁴ for $y = 0$ and 0.3 , respectively.

The absence of a C' contribution in the low-temperature specific heat of the AFM 2D metal $\text{Pr}_{0.5}\text{Sr}_{0.5}\text{MnO}_3$ confirms that this anomalous contribution is not of magnetic (AFM) origin and is present only in the CO state, in agreement with our previous findings [9–11]. Other experiments will be required to determine the origin of the excitations producing the C' contribution to the specific heat of charge-ordered material.

As the concentration of the Ca increases, the specific heat becomes larger (Fig. 3a). As suggested by the resistivity data (Fig. 1a), this can be an indication for two-phase coexistence in this system. If we express the specific heat of the intermediate compositions as $C_{\text{tp}}(T) = f_{\text{CO}}C_{\text{PCMO}} + (1 - f_{\text{CO}})C_{\text{PSMO}}$, where f_{CO} is the volume fraction of the CO phase, C_{PCMO} is the specific heat of the charge-ordered $\text{Pr}_{0.5}\text{Ca}_{0.5}\text{MnO}_3$, and C_{PSMO} is the specific heat of AFM 2D metal $\text{Pr}_{0.5}\text{Sr}_{0.5}\text{MnO}_3$, we find a reasonable quantitative fit to the experimental data (the dashed lines in Fig. 3b). The volume fractions of the CO phase, $f_{\text{CO}}(y = 0.8) = 0.8$, $f_{\text{CO}}(y = 0.6) = 0.48$, and $f_{\text{CO}}(y = 0.3) = 0.25$, appear to be close to the Ca content y . This demonstrates plausibility for two-phase coexistence. However, as seen in Fig. 3b, $C_{\text{tp}}(T)$ does not give an exact agreement with the experimentally observed specific heat. This is not unexpected, since the nature of phase separation in this compound is electronic (not chemical), and the presence of the Sr ion modifies the CO phase, while the presence of the Ca ion modifies the charge disordered phase (AFM 2D metal). We have observed similar behavior of the specific heat in the phase separated $(\text{La}_{1-y}\text{Pr}_y)_{0.67}\text{Ca}_{0.33}\text{MnO}_3$ system [11].

Now we discuss the effect of a magnetic field on the low-temperature specific heat of $\text{Pr}_{0.5}\text{Sr}_{0.5}\text{MnO}_3$ ($y = 0$). If $y = 0$ sample is cooled in a magnetic field of 7 T, which stabilizes the FM phase, the material remains in the FM metallic state [20], and the transition to the less conductive AFM state does not occur. We measured the specific heat of this field induced metallic state after the sample was cooled in the presence of a magnetic field of 8.5 T (Fig. 4). The specific heat in the magnetic field is significantly larger than the zero field specific heat. The increase of the specific

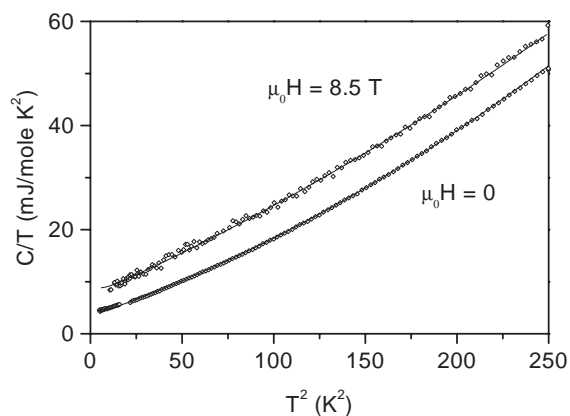


Fig. 4. Low-temperature specific heat of $\text{Pr}_{0.5}\text{Sr}_{0.5}\text{MnO}_3$ plotted as C/T vs. T^2 in zero and 8.5 T (field cooled) magnetic fields. Lines are fits described in text.

heat of $\text{Pr}_{0.5}\text{Sr}_{0.5}\text{MnO}_3$ in a magnetic field at a fixed temperature of 5 K was observed previously [21]. Since the sample is in the FM state at this magnetic field, we should include in Eq. (2) the FM spin-wave contribution

$$C_{\text{FM}}(T, H) = \frac{k_{\text{B}}(k_{\text{B}}T)^{3/2}}{4\pi^2 D^{3/2}} \times \int_{g\mu_{\text{B}}H/k_{\text{B}}T}^{\infty} \frac{x^2 e^x}{(e^x - 1)^2} \left(x - \frac{g\mu_{\text{B}}H}{k_{\text{B}}T}\right)^{1/2} dx,$$

where D is the spin-wave stiffness [22]. The best fit to our data requires $C_{\text{FM}}(T, H) = 0$. However, as was noted in previous work [17,23], it is difficult to resolve the FM spin-wave contribution to the specific heat in FM metallic manganites due to its small value and the presence of the γT contribution. To estimate the spin-wave contribution to the specific heat the value of the spin-wave stiffness D is required. We are not aware of experimental data or theoretical calculations giving the value of D for $\text{Pr}_{0.5}\text{Sr}_{0.5}\text{MnO}_3$ in magnetic field. Therefore, we calculate $C_{\text{FM}}(T, H)$ using the spin-wave stiffness value $D = 170 \text{ meV \AA}^2$ obtained from neutron scattering [24] for another manganite, $\text{La}_{0.7}\text{Ca}_{0.3}\text{MnO}_3$. Using this assumption, the estimated value of the spin-wave contribution in magnetic field of 8.5 T was found to be less than 1.5% of total specific heat for all temperatures in a magnetic field of 8.5 T. This is smaller than the resolution limit of our experiment. Therefore, we do not include $C_{\text{FM}}(T, H)$ in our fit to the data of Fig. 4.

The fit parameters for the data of Fig. 4 are given in Table 1. We find the 8.5 T value of γ to be 4 mJ/mol K² larger than zero field value. This increase of γ , and therefore the density of states at the Fermi level $N(E_F)$, can be attributed to a transition from a 2D metallic state in zero field to a field induced 3D metallic state. This dimensional crossover was observed in an optical conductivity study of Pr_{0.5}Sr_{0.5}MnO₃ [5]. An increase of γ due to a 2D–3D transition in the magnetic field was also observed in the A-type antiferromagnet La_{0.51}Sr_{0.49}MnO₃ [18]. The density of states increases in magnetic field by the factor of 1.4 in the case of La_{0.51}Sr_{0.49}MnO₃, while we observed an increase by a factor of 2.2 in Pr_{0.5}Sr_{0.5}MnO₃. In zero magnetic field the La_{0.51}Sr_{0.49}MnO₃ is on the compositional boundary between the 3D and 2D metallic states. Perhaps a fraction of the 3D metallic phase exists in this material even in zero field, which increases zero-field value of γ , and makes the field induced enhancement of γ smaller than what we found for Pr_{0.5}Sr_{0.5}MnO₃.

4. Conclusions

We have studied the resistivity, magnetization, and low-temperature specific heat of Pr_{0.5}(Sr_{1-y}Ca_y)_{0.5}MnO₃ ($0 < y < 1$), which transforms from CO insulator to AFM 2D metal as y decreases. The compositions with low Ca content exhibit a specific heat consistent with their metallic nature, while compositions with higher Ca content have an anomalous excess specific heat present in CO state. For the concentration region between 0 and 1, we have found the evidence of the CO and AFM 2D metallic phase coexistence in Pr_{0.5}(Sr_{1-y}Ca_y)_{0.5}MnO₃. For Pr_{0.5}Sr_{0.5}MnO₃, we have found a large increase of the density of states at the Fermi level due to a crossover from 2D to 3D metal in an external magnetic field.

Acknowledgements

We thank A. Millis for helpful discussions and R.M. Headley for the experimental help. This

work is supported in part by the Maryland/Rutgers NSF-MRSEC, DMR #00-80008.

References

- [1] C.H. Chen, S.-W. Cheong, Phys. Rev. Lett. 76 (1996) 4042;
- Z. Jirak, et al., J. Magn. Magn. Mater. 53 (1985) 153.
- [2] H. Kawano, R. Kajimoto, H. Yoshizawa, Y. Tomioka, H. Kuwahara, Y. Tokura, Phys. Rev. Lett. 78 (1997) 4253.
- [3] T. Akimoto, Y. Maruyama, Y. Moritomo, A. Nakamura, K. Hirota, K. Ohoyama, M. Ohashi, Phys. Rev. B 57 (1998) R5594.
- [4] Y. Tokura, N. Nagaosa, Science 288 (2000) 462.
- [5] J.H. Jung, H.J. Lee, T.W. Noh, Y. Moritomo, Y.J. Wang, X. Wei, Phys. Rev. B 62 (2000) 8634.
- [6] R. Bachmann, F.J. Disalvo Jr., T.H. Geballe, R.L. Greene, R.E. Howard, C.N. King, H.C. Kirsch, K.N. Lee, R.E. Schwall, H.-V. Thomas, R.B. Zubeck, Rev. Sci. Instrum. 43 (1972) 205.
- [7] J. Hejtmanek, Z. Jirak, Z. Arnold, M. Marysko, S. Krupicka, C. Martin, F. Damay, J. Appl. Phys. 83 (1998) 7204.
- [8] D. Niebieskikwiat, R.D. Sanchez, A. Caneiro, B. Alascio, Phys. Rev. B 63 (2001) 212402.
- [9] V.N. Smolyaninova, K. Ghosh, R.L. Greene, Phys. Rev. B 58 (1998) R14725.
- [10] V.N. Smolyaninova, Amlan Biswas, X. Zhang, K.H. Kim, Bog-Gi Kim, S.-W. Cheong, R.L. Greene, Phys. Rev. B 62 (2000) R6093.
- [11] V.N. Smolyaninova, A. Biswas, P. Fournier, S. Lofland, X. Zhang, Guo-meng Zhao, R.L. Greene, Phys. Rev. B 65 (2002) 104419.
- [12] B.F. Woodfield, M.L. Wilson, J.M. Byers, Phys. Rev. Lett. 78 (1997) 3201.
- [13] J.E. Gordon, et al., Phys. Rev. B 59 (1999) 127.
- [14] P.W. Anderson, B.I. Halperin, C.M. Varma, Philos. Mag. 25 (1971) 1;
- W.A. Phillips, J. Low Temp. Phys. 7 (1972) 351.
- [15] A.K. Raychaudhuri, A. Guha, I. Das, R. Rawat, C.N.R. Rao, Phys. Rev. B 64 2001 (165111).
- [16] E.A. Turov, Physical Properties of Magnetically Ordered Crystals, Academic Press, New York, 1965.
- [17] J.J. Hamilton, E.L. Keatley, H.L. Ju, A.K. Raychaudhuri, V.N. Smolyaninova, R.L. Greene, Phys. Rev. B 54 (1996) 14926.
- [18] Y. Moritomo, T. Akimoto, H. Fujishiro, A. Nakamura, Phys. Rev. B 64 (2001) 064404.
- [19] F. Damay, Z. Jirak, M. Hervieu, C. Martin, A. Maignan, B. Raveau, G. Andre, F. Bouree, J. Magn. Magn. Mater. 190 (1998) 221.
- [20] Y. Tomioka, A. Asamitsu, Y. Moritomo, H. Kuwahara, Y. Tokura, Phys. Rev. Lett. 74 (1995) 5108.

- [21] M. Roy, J.F. Mitchell, S.J. Potashnik, P. Schiffer, *J. Magn. Magn. Mater.* 218 (2000) 191.
- [22] C. Kittel, *Quantum Theory of Solids*, Wiley, New York, 1964.
- [23] L. Ghivelder, I. Abrego Castillo, N.McN. Alford, G.J. Tomka, P.C. Riedi, J. MacManus-Driscoll, A.K.M. Akther Hossain, L.F. Cohen, *J. Magn. Magn. Mater.* 189 (1998) 274;
- M.R. Lees, O.A. Petrenko, G. Balakrishnan, D.M. Paul, *Phys. Rev. B* 59 (1999) 1298.
- [24] J.W. Lynn, et al., *Phys. Rev. Lett.* 76 (1996) 4046.